



# A Low-Power, High-Gain Amplifier with Rail-to-Rail Operating Capability: Applications to Biomedical Signal Processing

Hassan Faraji Baghtash\*, and Rasoul Pakdel

Faculty of Electrical Engineering, Sahand University of Technology, Sahand New Town,  
Tabriz, Iran

**Abstract:** A low-voltage, low-power, rail-to-rail, two-stage trans-conductance amplifier is presented. The structure exploits body-driven transistors, configured in folded-cascode structure. To reduce the power consumption, the transistors are biased in the subthreshold region. The Specter RF simulation results which are conducted in TSMC 180nm CMOS standard process proves the well-performance of the proposed structure. The performance of the proposed structure against process variations is checked through process corners and Monte Carlo simulations. The results prove the robustness of the proposed amplifier against process uncertainties. Some important specifications of the design derived from circuit simulations are 93.36 dB small-signal gain, 14.4  $PV^2/Hz$  input referred noise power, 26.5 kHz unity gain frequency, 20 V/ms slew rate. The proposed structure draws 260 nW power from 0.5 V power supply and is loaded with a 15 pF loading capacitor. The input common mode range of structure is from 0 to 0.5 V.

**Keywords:** Body-driven, Low-power, Sub-threshold, Low-voltage, Folded Cascade Structure.

## 1. INTRODUCTION

Today, the request for low-power, low-voltage, battery-operated circuits and systems is increased drastically. Numerous efforts have been made to lower the supply voltage of the structures. This trend is mainly imposed by technology scaling, from one generation to another, following Moore's scaling law. This trend also is encouraged by the increased versatility of battery-powered and portable devices [1, 2]. Emerging applications such as implantable medical devices, which need to operate with extremely low power dissipation ( $P_{diss}$ ), made low voltage and low power circuit design more interesting than ever.

In the reduced supply voltages, using transistors operating in the subthreshold region is a very good choice, because they inherently overcome the threshold voltage limitation associated with regular application of transistors in the saturation region. Besides, as they have high  $gm/I$  ratio, they deliver high efficiency in terms of power consumption, as well.

The operational amplifiers are amongst the most important analog building blocks. As the logic gates in digital circuitries, the OTAs play very critical role in analog circuit and system designs [3]. For amplifiers, there are very common well-known features, of which some are more important in the biomedical applications. A number of these characteristics are: high common-mode rejection ration (CMRR), low input-referred noise (IRN), and low power consumption. The high value of CMRR is mandatory to remove the DC offsets from biological signals. The low noise operating performance is also essential due to the fact that the weak biological signals are always surrounded by a very noisy world. Finally, the power consumption must be kept in the range; as the device is usually in direct contact with the body, hence the heat from the high power consumption may damage the body or the organs in contact with the system [4].

Some efforts have been made to design the amplifier with the abovementioned conditions. For instance, a differential amplifier with devices operating in sub-threshold region is presented in

[3] to achieve the low power consumption. In [4], the PMOS input transistors are used alongside the switched biasing method to lower the area and IRN. In [5], the body-driven transistors are adopted in folded cascode structure in order to satisfy the design demands.

Literature review reveals that it is not so hard to achieve high gain or high CMRR in a reduced power consumption design. However, it is really difficult to design a high-speed but low-power operational amplifier. The reason behind this is that there is always a tradeoff between the power consumption and speed of operation in operational amplifiers. The [3] tries to maximize the unity-gain frequency (UGF) over power dissipation (UGF/ $P_{diss}$ ). The paper succeeds to reach the defined figure of merit (FOM) and presents a circuit operating with considerably low power consumption. However, the examinations are done with a very low load capacitance of 0.5 pF, which is at least 30 times less than that's used by similar works. The challenge is dealt with in some recent works, trying to push the borders much further away. For example, in [6-10] body-driven technique is employed to enable low-voltage low-power operation of structures. They all show excellent performance and perform well in very reduced power supplies. Nevertheless, the power consumption is still so high for some energy aware applications such as implantable medicals.

Here, in this work, we present a low-voltage, low-power amplifier structure that tries to boost the unity-gain frequency over power dissipation. Utilizing a PMOS bulk-driven input stage configured in the folded cascode structure, the proposed structure succeeds to reach most of the

design parameters. The presented circuit operates properly in the entire input common-mode range (ICMR), providing a full common mode swing range from negative to positive supply rails. The simulation results show that the presented OTA outperforms most similar works in terms of supply voltage, DC gain ( $G_0$ ), and provided FOM.

The paper is arranged in four sections. After section 1 which introduce the paper, section 2 explains the proposed OTA, the simulation results are given in section 3. In the end, section 4 concludes the paper.

## 2. THE PROPOSED AMPLIFIER

The transistor level realization of the proposed OTA is depicted in Figure 1. The circuit is constructed from an input stage, a gain stage and an output stage (regions I, II, and III in Figure. 1, respectively). The input stage is designed such that it can offer full common-mode voltage swing from ground to positive supply rail. This is accomplished through bulk-driven input transistors of M1-M2. Normally, in traditional designs, using bulk-driven transistors is not an interesting choice, as it offers less gain-bandwidth product due to the reduced trans-conductance of transistors. However, for the target application of the proposed structure that needs very less gain bandwidth product, it is not a concern at all [11, 12]. In other word, in the biomedical applications, bulk-driven transistors are preferred over gate-driven ones as they offer less trans-conductance variation over input common-mode range. The flicker noise of the structure is handled by employing the large PMOS input transistors instead of NMOS transistors.

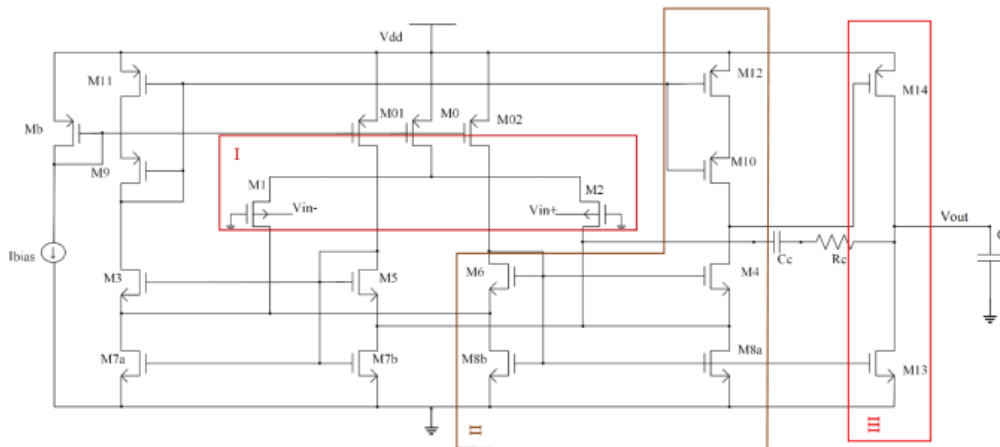


Fig. 1. The transistor-level realization of the proposed OTA

The biasing of the structure is provided by biasing current of 'Ibias' and bias transistors of Mb, M0, M01-M02. Transistors M3-M12 configure six composite transistors which effectively collect the injected current signals from M1-M2, perform amplification, and deliver the amplified signals to the output stage. The composite transistors enable the structure to receive the current signals from input stage and deliver them to the output stage with minimum voltage requirement and increased output impedance and current transfer accuracy. The output stage of the structure is accomplished through a common output stage. All devices are operating in sub-threshold region to deliver the maximum  $g_m/I_D$  ratio.

Examining the proposed amplifier, the following equations can be derived, formulating some small signal parameters of the design.

$$A_{dm} = \frac{(N+1)g_{mb1}g_{m14}}{(g_{o13} + g_{o14})(L+K)} \quad (1)$$

where  $A_{dm}$  is the DC differential voltage gain,  $N$  is the mirroring ratio between M7a and M7b or M8a and M8b, and  $L$  and  $K$  are given by:

$$L = \frac{g_{o4}(g_{m5} + g_{mb5} + G_O)}{g_{m4} + g_{mb4} + g_{m5} + g_{mb5} + g_{o4} + G_O},$$

$$G_O = g_{o1} + g_{o2} + g_{o5} + g_{o7b} + g_{o8a} \quad (2)$$

$$K = \frac{g_{o10}g_{o12}}{g_{m10} + g_{mb10} + g_{o10} + g_{o12}} \quad (3)$$

The common mode gain can be calculated as:

$$A_{cm} = G_{MX} \times \frac{g_{o0}}{g_{o0} + g_{mb1} + g_{mb2}} \times \frac{g_{m4}g_{m10}g_{m14}}{(g_{o13} + g_{o14})(g_{m7b}g_{o4}g_{o10} + g_{m4}g_{o10}g_{o14})} \quad (4)$$

$$G_{MX} = \frac{g_{mb1}}{g_{m8b} + g_{m3}} \left( g_{m8a} - g_{m3} \frac{g_{m12}}{g_{m11}} \right) + \frac{g_{mb2}}{g_{m4} + g_{m7b}} \left( g_{m4} - g_{m7a} \frac{g_{m12}}{g_{m11}} \right) \quad (5)$$

Finally, the CMRR can be calculated as:

$$CMRR = \frac{A_{dm}}{A_{cm}} \quad (6)$$

The equation (5) reveals that the CMRR can be reach infinity providing that can be satisfied.

$$\frac{g_{m8a}}{g_{m3}} = \frac{g_{m4}}{g_{m7a}} = \frac{g_{m12}}{g_{m11}}$$

### 3. SIMULATION RESULTS AND DISCUSSIONS

The simulations are carried out using TSMC 180 nm, MS/RF, 1P6M, CMOS technology utilizing Spectre RF simulator. The amplifier is biased with a 0.5 V power supply and loaded with a 15 pF capacitor ( $C_L$ ). The bias currents and device sizes that are used in circuit simulations are given in Table 1.

Open loop frequency performance of the proposed OTA is pictured at Figure. 2. As depicted in this Figure, the open loop gain is 93.36 dB and the amplifier delivers the unity-gain bandwidth of 26.5 kHz with a 60o phase margin. Fortunately, the obtained DC gain and UGF cover the system requirements in most biomedical implants.

One of the most important parameters of amplifiers in biomedical applications is CMRR. Interestingly, the proposed structure presents more than 128 dB CMRR which is shown in Figure 3. Willingly, the 3-dB bandwidth of the CMRR is about 20 Hz which is rather high and acceptable for most of biomedical applications. This high value of CMRR is due to the balanced configuration of the proposed structure which suppress the common mode signals effectively. This also confirms the discussions from (4) and (6).

**Table 1.** Transistors Sizing and Element Value

Element	Value ( $\mu\text{m}/\mu\text{m}$ )	Element	Value ( $\mu\text{m}/\mu\text{m}$ )
Mb	150/3	M9, M10	380/1.6
M0	450/3	M11, M12	185/3
M01, M02	60/9	M13	180/1.5
M5, M6	19.2/5	Cc	4.5 pF
M7a, M8a	73/3	Rc	700 K $\Omega$
M7b, M8b	30/3	Ibias	35 nA

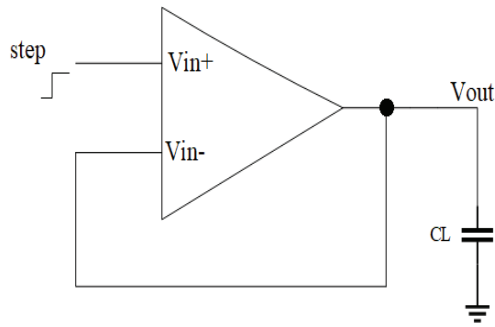


Fig. 6. Unity-gain feedback configuration

The IRN parameter for the OTA structure is pictured in Figure 4. From this figure, it is noticeable that  $1/f$  noise dominates at low frequencies, whereas, in higher frequencies, it is the thermal noise that plays the main role. The input referred noise is evaluated to be  $14.14 \text{ pV}^2/\text{Hz}$  at the core frequency of 1 Hz, which is an acceptable value for most the biomedical applications.

To ensure the full range operation, the input common-mode range is investigated. As shown in Figure 5, the output voltage experiences a full rail-to-rail swing (from 0 to 500 mV) while the input voltage varies from negative rail to the positive rail. This rail-to-rail input common mode range is indeed essential in low-voltage circuits with reduced voltage swing ranges.

To examine the transient performance of the proposed amplifier, it is configured in a unity-gain feedback (see Figure 6) and a step voltage with

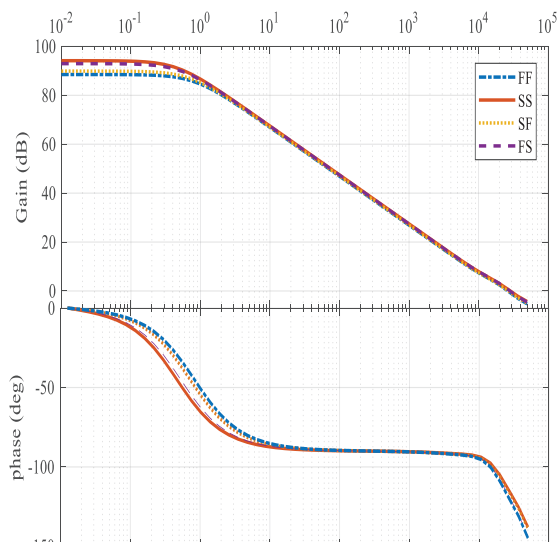


Fig. 8. The transient step response

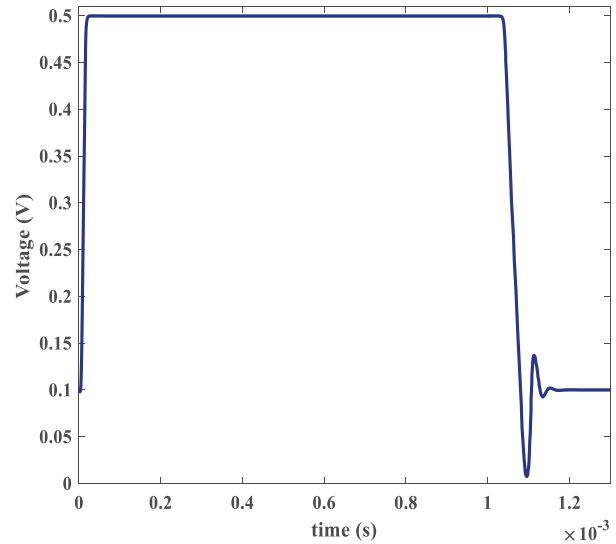


Fig. 7. The transient step response

the amplitude of  $0.9 \text{ V}_{pp}$  ( $100 \text{ mV} - 1 \text{ V}$ ) and frequency of 500 Hz is applied to its input node. The transient response is displayed in Figure. 7. This figure exhibits a settling time of  $75 \mu\text{s}$  and an average slew rate value of  $20 \text{ V/ms}$ .

Figure 8 shows the results of the corner simulations for the proposed amplifier. The frequency performance of OTA structure is examined in this figure. Some abstracts from this figure are given in Table 2. Fortunately, the results (from Figure 8 or Table 2) are promising as they confirm the robustness of the proposed circuit against process deviations.

Finally, the Monte Carlo simulations with 1000 runs are conducted to evaluate the robustness of

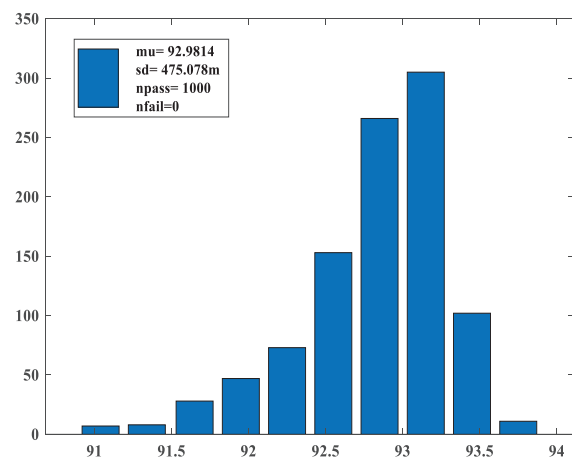


Fig. 9. The spectrum of voltage gain

**Table 2.** The OTA Parameters Comparison

parameter	This work	[17]	[16]	[15]	[14]	[13]	[12]	[5]	[4]	[3]
VDD (V)	0.5	0.5	0.5	0.5	0.8	0.9	0.6	0.6	±1.5	-
G <sub>0</sub> (dB)	93.36	83.58	65	67.8	59	70	73.5	80	76.2	48
CMRR (dB)	128.36	129	86	-	-	59	67.4	130.2	129.67	-
C <sub>load</sub> (pF)	15	15	20	15	25	20	15	15	7.5	0.5
UGF (kHz)	26.5	23.8	550	3.26	0.21	5.6	13.02	19.1	10.84	29
PM (°)	60	61.5	50	68.9	83	62	54.1	60	74	60
P <sub>diss</sub> (nW)	263.8	351	28000	26	40	450	550	400	15174	21
FOM (dB kHz pF/nW)	140.67	140	25.5	127.5	7.74	17.4	26.1	52.3	0.408	33.14
Technology (nm)	180	180	180	180	350	2500	350	180	180	90

**Table 2.** OTA Parameters in Four Operating Corners

OTA parameter	Corner			
	FF	FS	SF	SS
G <sub>0</sub> (dB)	88.5	92.94	89.88	94.14
PM (°)	60.75	60	64.2	63
UGF (kHz)	26.32	28.35	26.77	28.75

the circuit against process variations. To do this, the DC gain of the amplifier is examined. Figure 9 presents the results. For DC gain, the standard deviation and mean value extracted from Monte Carlo simulations are obtained to be 475.078 mdB and 92.9814 dB, respectively. The results show well-agreement with the results from the corner simulations, validating the circuit performance over process changes, further.

To fairly investigate the performance of proposed circuit with that's of other similar works, we used (7) as the figure of merit (FOM), which is adopted from [5]:

$$FOM = G_0 \times \frac{UGF}{P_{diss}} \times C_L \quad (7)$$

The functionality of the proposed structure is compared with that's of recent relevant circuits at Table 3. The results show better functionality of the presented structure at some important parameters such as Gain, UGF and FOM.

#### 4. CONCLUSION

A high-gain low-power body-driven folded-cascode OTA is presented in this work. The simulation results, proved the advantage and improved functionality of this work compared to other similar works. The results are validated with Spectre circuit simulator employing TSMC 180nm CMOS standard process. Due to the good characteristics of the proposed structure in terms of CMRR, noise, gain, and power consumption, it tenders itself well, for utility in low-voltage applications, especially in the processing of biological signals such as EEG and ECG signals.

#### 5. REFERENCES

1. H. Faraji Baghtash, K. Monfaredi, and A. Ayatollahi. A novel ±0.5 V, high current drive, and rail to rail current operational amplifier. *Analog Integrated Circuits and Signal Processing* 70: 103-112 (2012).
2. H. Faraji Baghtash and A. Ayatollahi. A high CMRR, class AB, fully differential current output stage. *Analog Integrated Circuits and Signal Processing* 78: 465-477 (2014).
3. S. Tyagi et al. A 21nW CMOS Operational Amplifier for Biomedical Application. in *Proceedings of the International Conference on Nano-electronics, Circuits & Communication Systems* 389-396 (2017).
4. D. Dubey and A. Gupta. A low power low noise amplifier for biomedical applications. in *2015 IEEE International Conference on Electrical, Computer and Communication Technologies (ICECCT)* 1-6 (2015).
5. M. Akbari and O. Hashemipour. A 0.6-V, 0.4-μW bulk-driven operational amplifier with rail-to-rail

- input/output swing. *Analog Integrated Circuits and Signal Processing, journal article* 86: 341-351 (2016).
6. H. Faraji Baghtash. A 0.4 V, tail-less, fully differential trans-conductance amplifier: an all inverter-based structure. *Analog Integrated Circuits and Signal Processing*, 104: 1-15 (2020).
  7. H. Faraji Baghtash. A 0.4 V, body-driven, fully differential, tail-less OTA based on current push-pull. *Microelectronics Journal* 99: (2020).
  8. H. Veldandi and R. A. Shaik. A 0.3-V Pseudo-Differential Bulk-Input OTA for Low-Frequency Applications. *Circuits, Systems, Signal Processing* 37: 5199-5221 (2018).
  9. F. Khateb, T. Kulej, M. Kumngern, and C. Psychalinos. Multiple-input bulk-driven MOS transistor for low-voltage low-frequency applications. *Circuits Syst Signal Process* 38: 2829-2845 (2019).
  10. T. Kulej and F. Khateb, "Design and implementation of sub 0.5-V OTAs in 0.18- $\mu$ m CMOS," *international Journal of Circuit Theory and Applications* 46: 1129-1143 (2018).
  11. Bashir, M., Patri, S. R., & KrishnaPrasad, K. S. R. 0.5 V, high gain two-stage operational amplifier with enhanced transconductance. *International Journal of Electronics Letters* 6(1): 80-89 (2018).
  12. Ferreira, L. H. C., Pimenta, T. C., & Moreno, R. L.. An Ultra-Low-Voltage Ultra-Low-Power CMOS Miller OTA With Rail-to-Rail Input/Output Swing. *IEEE Transactions on Circuits and Systems II: Express Briefs* 54(10): 843-847 (2007).
  13. Mourabit, A. E., Guo-Neng, L., & Pittet, P. Wide-linear-range subthreshold OTA for low-power, low-voltage, and low-frequency applications. *IEEE Transactions on Circuits and Systems I: Regular Papers* 52(8): 1481-1488 (2005).
  14. Cotrim, E., & Ferreira, L. C. An ultra-low-power CMOS symmetrical OTA for low-frequency Gm-C applications. *Analog Integr. Circuits Signal Process.* 71(2): 275-282 (2012).
  15. X. Zhao, H. Fang, T. Ling, and J. J. I. Xu. Transconductance improvement method for low-voltage bulk-driven input stage. *Integration the vlsi journal* 49: 98-103 (2015).
  16. M. Trakimas, S. J. A. I. C. Sonkusale, and S. Processing. A 0.5 V bulk-input OTA with improved common-mode feedback for low-frequency filtering applications. *Analog Integrated Circuits and Signal Processing, journal article* 59 (1): 83-89 (2009).
  17. Rasoul Pakdel, Hassan Faraji Baghtash. Design of a Low Noise Low Power Amplifier for Biomedical Applications. *2018 25<sup>th</sup> National and 3<sup>rd</sup> International Iranian Conference on Biomedical Engineering (ICBME)* (2018).